

Chapter 11

Robotic Platforms and Experiments

P. Arena, S. De Fiore, D. Lombardo and L. Patané

Abstract To reach the challenging objectives of the SPARK project the research pathway followed different levels of abstraction: mathematical models, insect behavior study and bio-inspired solutions for robotics. We investigated biological principles as a source of inspiration and we finally applied the mechanisms provided by the complex dynamical system theory to realize mathematical models for cognitive systems. All these aspects deeply investigated in previous Chapters, are here applied to solve specific tasks. A series of wheeled and legged robots are described and applied as test beds for the proposed action-oriented perception algorithms. The cognitive architecture has been experimentally tested at multiple levels of complexity in different robots. Details on the robotic platforms are given together with a description of the experimental results that include multimedia materials collected in the project web page.

11.1 Introduction

The complete model for action-oriented perception, that has been outlined in the previous chapters, is a modular architecture structured with parallel pathways and hierarchical structures. Basically the inspiration comes from the insect world even if the idea was not to biologically reproduce an insect brain model but to deeply understand insect cognitive behaviours for a possible implementation. The experimental phase was the last step of our activities, aiming at validate the proposed control system. The evaluation procedure was carried out both by using virtual agents working in dynamic simulation environments and with real robots. In particular to test at different levels of complexity the cognitive architecture, both wheeled and legged robots were designed, realized and used.

P. Arena, S. De Fiore, D. Lombardo and L. Patané
Department of Electrical, Electronic and System Engineering, University of Catania, I-95125 Catania, Italy, e-mail: [parena, lpatane]@diees.unict.it

In particular, when the whole complex perceptual architecture had to be tested, a dual drive wheeled structure was used, due to its simple structure and motion control strategy. On the other hands, the design and realization of legged machines was performed primarily to implement low level bio-inspired locomotion strategies, like the Central Pattern Generator and the decentralized locomotion control (Walknet). Of course, once the high level perceptual algorithms will be optimized and tested, these will be transferred from the wheeled to the legged machines to explore the emergence of perceptual algorithms from locomotion primitives.

Two roving platforms have been used for the demonstration: Rover I and II. The control architecture of both rovers consists in a low level layer based on micro-controllers that handle the motor system and a high level layer that includes the Eye-RIS visual system as a main controller together with the SPARK board. The rovers are also endowed with a suite of different sensors and can be interfaced with a PC through a wireless communication link.

As far as the legged structure is concerned, mainly two different robots have been developed. The former is called MiniHex. It is a mini-hexapod robot with 12 DoF controlled with a Central Pattern Generator (CPG), realized with a CNN-based chip. The robot can be telecontrolled from a PC, but can also navigate autonomously showing phobic or attractive behaviours [6, 1] using three infrared distance sensors equipped on its head. The latter hexapod is called Gregor III. It is a cockroach-inspired legged robot and is the final prototype of a series. The core of the system is the SPARK board that handles the complex sensory system distributed on the robot. In Gregor III the locomotion control problem has been solved by using both a CPG and a reflex-based decentralized approach (based on Walknet) that has been exploited to realize climbing and turning strategies.

The experiments, discussed in this chapter, aim at demonstrate the applicability of the SPARK cognitive architecture analyzing some specific aspects of the model as for example: the basic behaviours (e.g. obstacle avoidance), proto-cognitive behaviours (e.g. visual homing), correlation mechanisms (e.g. learning anticipation through STDP), representation layer (e.g. Turing pattern approach to perception).

Eight different experiments are here presented, showing the objectives, the experimental set-up and the obtained results:

1. Visual homing and hearing targeting;
2. Reflex-based locomotion control with sensory fusion;
3. Visual perception and target following;
4. Reflex-based navigation based on WCC;
5. Learning anticipation via spiking networks;
6. Landmark navigation;
7. Turing Pattern Approach to perception;
8. Representation layer for Behaviour Modulation.

Multimedia materials on the robotic platforms and videos of the experiments are available on the SPARK Project web page [8].



Fig. 11.1 Rover I. (a) Configuration with the visual system in frontal position, (b) panoramic view configuration.

11.2 Robotic test beds: roving robots

11.2.1 Rover I

The roving robot *Rover I* is a classic four wheeled drive rover controlled through a differential drive system. The robot dimensions are 35 cm x 35 cm. Rover I is equipped with four infrared distance sensors GP2D12 from Sharp, with low level target sensors (i.e. able to detect black spots on the ground used as targets) and with an RF04 USB radio telemetry module for remote control operations and sensory acquisition. The detection range of the infrared sensors is set from 14 to 80 cm. A visual processor (i.e. Eye-RIS v1.1) can be equipped on the rover in two different configurations: in the front position for target aiming tasks (see Fig. 1(a)) and in a panoramic view configuration, obtained with a conic mirror, for homing purposes (see Fig. 1(b)). The control architecture is shown in Fig. 11.2: the core of the system is the visual processor Eye-RIS v1.1 that can be used, in substitution of the more powerful SPARK board, to implement simple pre- proto-cognitive behaviours. A I2C bus interfaces the visual processor with an ADC board that handles all the other sensory systems: distance sensors, hearing chip, low level target sensors and a battery pack control device. The robot is equipped with two 12V 3.5A batteries that guarantee an autonomy of about 1.5 hours; moreover a control system to monitor the battery charge level is implemented together with a recharging mechanism that extends the autonomy of the system in case of time consuming learning sessions.

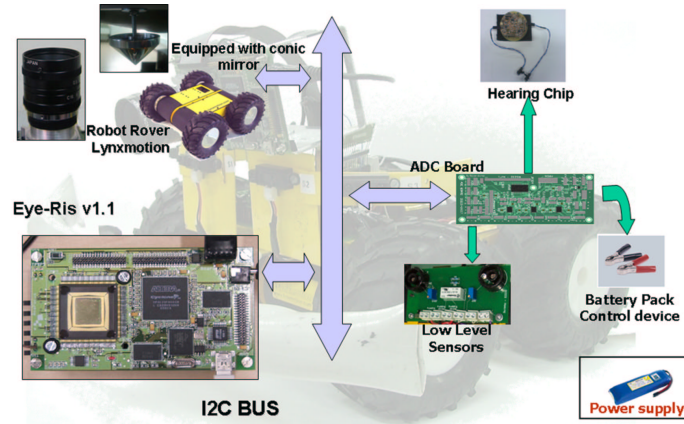


Fig. 11.2 Rover I control architecture.



Fig. 11.3 Rover II.

11.2.2 Rover II

Rover II, shown in Fig. 11.3, is an optimized version of Rover I. It is equipped with a bluetooth telemetry module, four infrared short distance sensors Sharp GP2D120 (detection range 3 to 80 cm), four infrared long distance sensors Sharp GP2Y0A02 (maximum detection distance about 150 cm), a digital compass, a low level target detection system, an hearing board for cricket chirp recognition and with the Eye-RIS v1.2 visual system.

The complete control architecture, reported in Fig. 11.4, shows how the low level control of the motors and the sensor handling are realized through a microcontroller STR730. This choice optimizes the motor control performances of the robot maintaining in the SPARK board and in the Eye-RIS visual system the high level cognitive algorithms. Moreover Rover II can be easily interfaced with a PC through a

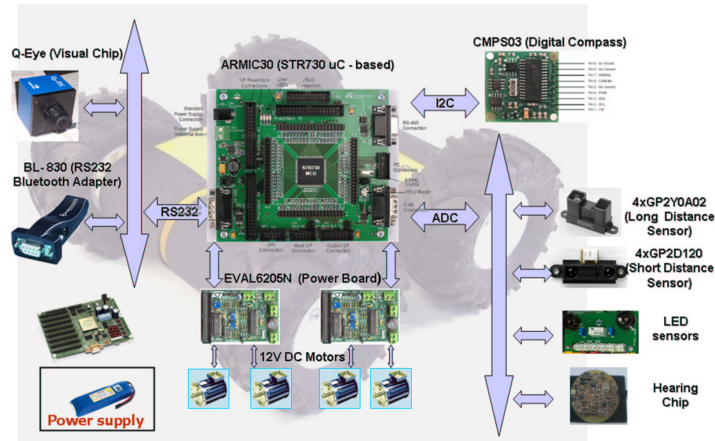


Fig. 11.4 Rover II control architecture.

bluetooth module: this remote control configuration allows to perform some preliminary tests debugging the results directly on the PC.

11.3 Robotic test beds: legged robots

11.3.1 MiniHex

The MiniHex robot, shown in Fig. 11.5 is a hexapod robot whose dimension are $15 \times 10 \times 10 \text{ cm}^3$ [2]. It is a legged mini-robot with 12 degrees of freedom actuated with the HS-85MG metal gear servo, which have a weight of 22g each and a stall torque of 3 kg-cm.

The architecture, endowed on the robot, is completely devoted to suitably control all the robot actuators for locomotion purposes. The generation of the locomotion patterns is assolved by a CNN-based VLSI CPG chip realized with the switched-capacitor (SC) technique that permits a stepping frequency regulation by using an external clock. The MiniHex is also autonomous from the power supply point of view. The servomotors are supplied with a pack of four AA Ni-MH batteries at 1.5 V whereas the chip and the electronics are sustained by two 9V batteries stabilized through a voltage regulator.

The robot can work in an autonomous configuration using three distance sensors for obstacle avoidance and target following tasks. It can be also tele-controlled thanks to a wireless communication module equipped on board.

The robot speed is in a range between 1 cm/s and 10 cm/s. The robot autonomy is estimated in a range between 0.5-1h on a flat terrain. Power consumption ranges between 10 W during walking on even terrain and 15 W during obstacle course.

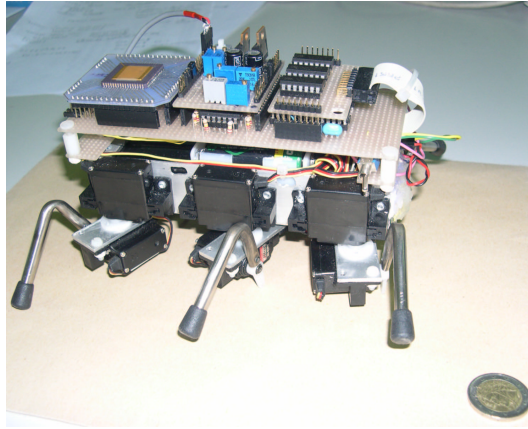


Fig. 11.5 MiniHex.

11.3.2 Gregor III

The hexapod Gregor III is the final prototype of the Gregor series. The robot, as shown in Fig. 11.6, is equipped with a distributed sensory system. The robot's head contains the Eye-RIS v1.2 visual processor, the cricket inspired hearing circuit and a pair of antennae developed using Ionic Polymer-Metal Composite (IPMC) material. A compass sensor and an accelerometer are also embedded in the robot together with four infrared distance sensors used to localize obstacles. A set of distributed tactile sensors (i.e. contact switches) is placed in each robot leg to monitor the ground contact and to detect when a leg hits with an obstacle.

The core of the control architecture is the SPARK board, as shown in Fig. 11.7. The robot sensory system is handled with an ADC board that is addressed by using an I2C bus, whereas the Eye-RIS v1.2 is interfaced with the main board through a dedicated parallel bus. The robot is completely autonomous for the power supply. Two 11.1V, 8A Li Poly battery packs are used: one for the motors and the other for the electronic boards.

The robot can be used as a walking lab able to acquire and process in parallel a huge amount of different types of data. For monitoring the system status and for storing purposes, a wireless module is used to transmit the sensible information to a remote PC (see Fig. 11.8).

11.4 Experiments and results

11.4.1 Visual homing and hearing targeting

Objectives: This demo aims at proving the reliability of the Rover I robot endowed with algorithms implementing both visual and hearing routines and related circuits.

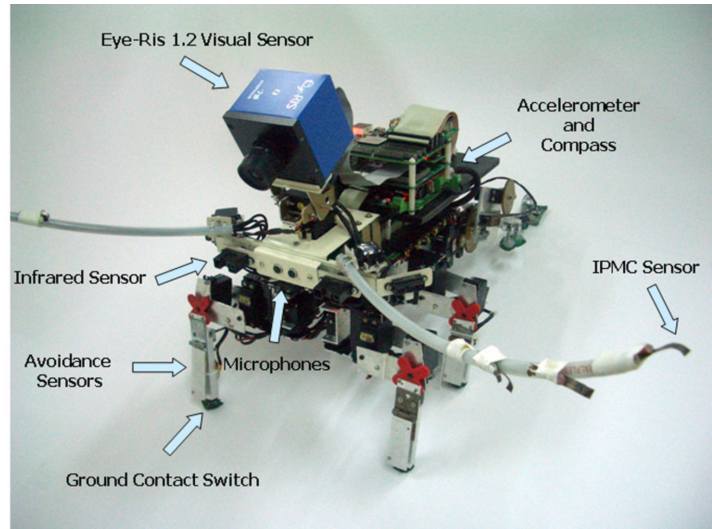


Fig. 11.6 GregorIII.

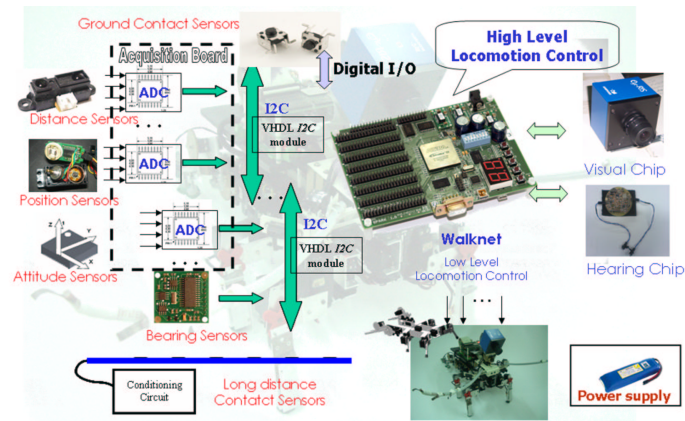


Fig. 11.7 GregorIII control architecture.

The task to be accomplished consists in a phonotaxis behaviour performed until the battery level goes under a warning threshold. In this condition, the system triggers a basic behaviour “inherited” for survival purposes: *homing*. In the proposed experiment the robot adopts a visual homing behaviour using the visual system in a panoramic configuration.

Experimental set-up: The robot moves in a $3 \times 3 \text{ m}^2$ arena, attracted by the sound sources that reproduce the cricket calling song. Two speakers are placed near two opposite walls, whereas a recharging station is located in a corner of the arena. Rover I is equipped with: Eye-RIS v1.1 in a panoramic configuration, hearing cir-

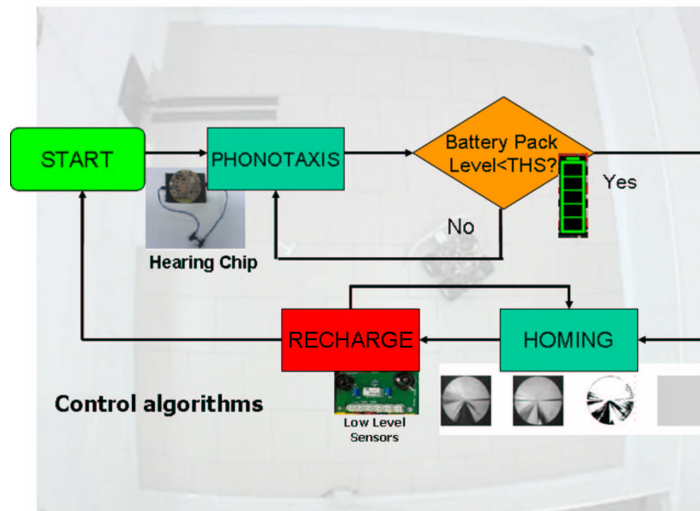


Fig. 11.9 The Rover I, equipped with the Eye-RIS 1.1 in a panoramic configuration and the hearing board, performs an hearing and visual homing task. The robot is attracted by the cricket calling song but when the battery level is dangerously low, the homing behaviour is triggered to find the recharging station.

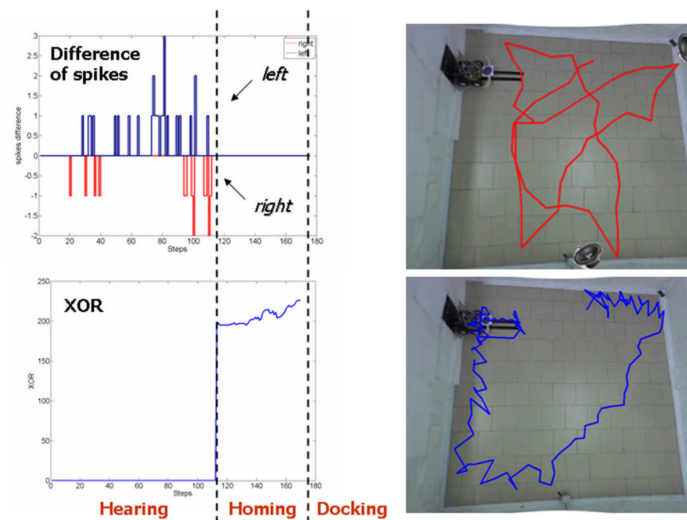


Fig. 11.10 Results of the hearing targeting and homing experiment.

When the homing procedure is activated, the home image is compared with the actual image. The direction to be followed is obtained using a gradient-based algorithm that is developed inside the Eye-RIS v1.1 device and is based on the XOR function (for details see [3]). Following the ascending direction of the XOR-based

index, as shown in Fig. 11.10, the robot can find the recharging station position. When the low level sensors detect black strips on the ground, the homing algorithm is stopped.

Docking: the homing phase is followed by a docking procedure that is needed to connect the recharging plates equipped on the robot with the station. Two black lines on the ground indicate the position of the connectors in the base station. Using two photo-diodes the robot can find the position of the lines and perform the docking. A micro-switch detects the connection and activates the recharging circuits: at the end of the process the battery level system stimulates the phonotaxis behaviour again.

Data acquired during an experiment are reported in Fig. 11.10. The homing mechanism is here activated after two targets retrieving.

11.4.2 Reflex-based locomotion control with sensory fusion

Objectives: This demo aims at proving the reliability of the reflex-based Walknet controller for Gregor III [7, 4]. Tactile sensors will be used for autonomous navigation and obstacle climbing.

Experimental set-up: The arena used for the experiments is the same of the previous demo with the inclusion of several obstacles that can be avoided or climbed. The hexapod platform, Gregor III, is endowed with: distributed tactile sensors, IPMC-based antennal sensor, distance sensors, an accelerometer, the hearing board and the visual processor Eye-RIS v1.2.

Results:

The hexapod robot Gregor III has been designed as a moving laboratory used to test the bio-inspired locomotion principles introduced in Chapter 2. The robot equipped with a Li-Poly battery pack, can walk autonomously for about 30 minutes, exchanging data with a remote workstation through a wireless communication link.

When the robot stability is compromised during an experiment, a recovery procedure is performed. Dangerous situations are detected using a posture controller implemented through a three-axis accelerometer equipped on board.

Fig. 11.11 shows two different scenarios used to test the robot capabilities for autonomous navigation in cluttered environments and obstacle climbing.

Further experiments have been performed on the Gregor III to deeply analyze other sensing capabilities as for instance the auditory system. The cricket-inspired hearing board, equipped on the robot, has been used to test the basic behaviour of phonotaxis. Due to the complexity of the robot structure, an analysis of the disturbances introduced by the 20 servomotors (i.e. 16 for the legs and 4 for the antennae) was carried on. The results, reported in Fig. 11.12, show how the sound recognition system, even if affected by the noise introduced by motors, easily permits to identify the sound source location.



Fig. 11.11 Walknet on Gregor III. (a) Obstacle climbing, (b) autonomous navigation in a cluttered environment.

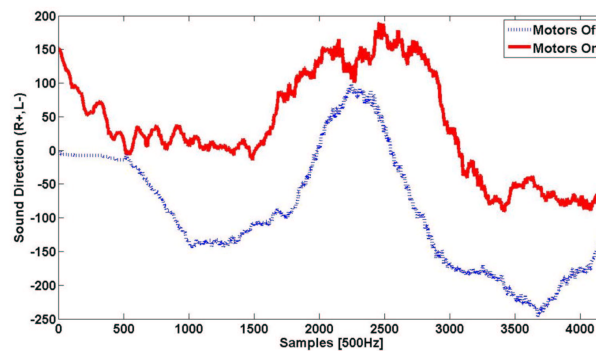


Fig. 11.12 Output of the hearing circuit, adopting a sample frequency of 500Hz and after a 1 Hz low pass filter. The sound source diffusing the cricket calling song is initially located in front of the robot and then is moved on the left, afterwards on the right and finally another time on the left of the robot. The disturbance introduced by motors is evident but the source direction can be easily distinguished.

11.4.3 Visual perception and target following

Objectives: This demo is focused on the application of visual perceptual algorithms on Rover II.

Experimental set-up: Rover II and MiniHex are placed in a $3 \times 3 m^2$ arena filled with different objects. The visual processor Eye-RIS v1.2 equipped on the rover is used to detect the presence of the MiniHex and to follow it while moving in the arena.

Results:

This demo emphasizes the processing capabilities of the Eye-RIS v1.2 system. The visual system, equipped on Rover II is able to process in real-time the images acquired by the robot aiming at recognizing the presence of the MiniHex robot among different other objects visible in the scene (see Fig. 11.13).

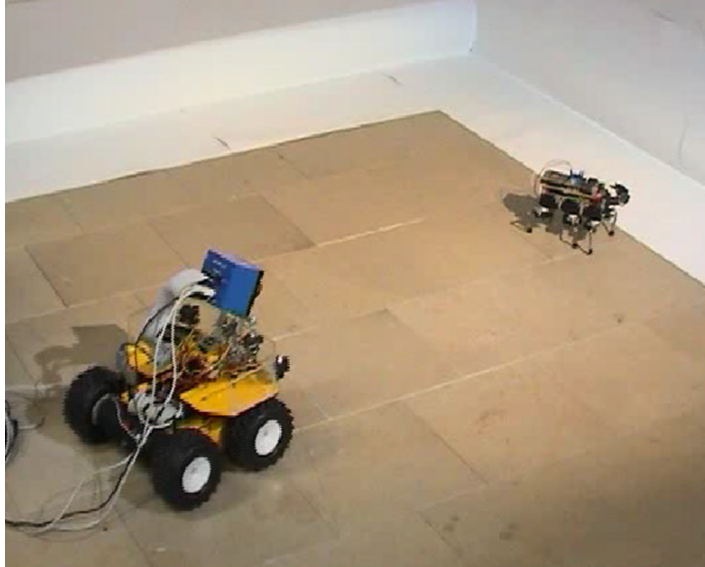


Fig. 11.13 The Rover II recognizes and follows the MiniHex.

The designed visual algorithm is based on a sequence of operators that deeply exploit the parallel processing capabilities of the system. In Fig. 11.14, the output of each step executed within the interframe rate (about $30ms$) is given. A gaussian filter together with some MAC operations is applied to the acquired image to increase the contrast in order to easily identify the different objects in the scene. A dynamic threshold is then used to eliminate the background from the image and a mask is applied to leave out the edge from the processing avoiding to process objects that are only partially seen in the acquired image. Templates for erosion and dilation are successively applied to filter noise and fill holes creating well defined blobs. The position of each blob is then obtained by using the centroid operator. The dimensions of the blobs can be also found tracing horizontal and vertical lines starting from the centroid, making a logical operator with the output of the erosion and dilation step, and finally counting the number of pixels. The ratio between the horizontal and vertical dimension of each object is then used as a characteristic feature to identify the MiniHex robot in the scene. The addition of further filtering functions can enhance the detection of the detection of the MiniHex structure among different kinds of objects.

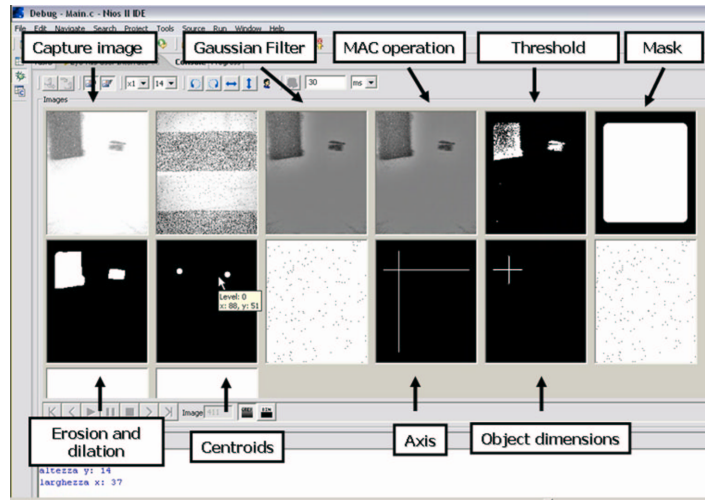


Fig. 11.14 Image processing on Eye-RIS 1.2.

11.4.4 Reflex-based navigation based on WCC

Objectives: A chaotic system is applied to navigation control in a roving robot. The reflexive strategy, based on the weak chaos control technique (WCC), is compared with other standard methods like the potential field.

Experimental set-up: The experimental platform is constituted by the SPARK board that implements the navigation algorithm, a mobile robot and a wireless communication system. A computer can be used to make a backup of the data for a post process analysis. See reference [5] for details on the implementation aspects. Rover I, equipped with four distance sensors, is used in these experiments. The aim is to underline the obstacle avoidance and exploration capabilities of the roving robot. For these reasons, different types of arenas have been considered.

Results:

The robot sensory system, that represents the input of the control system, is directly linked to the cycle used to enslave the chaotic system as discussed in Chapter 6.

Considering the sensor positions and orientations (Fig. 11.15), sensor S_i is associated to the reference cycle Ref_i . Sensors S_3 and S_4 have been configured in order to have a limited activation range with respect to the others. In this way the robot could pass through narrow spaces.

The NiosII microprocessor is devoted to the execution of the deterministic navigation algorithm and to the supervision of the activity of the VHDL entity implementing the weak chaos control. The WCC process lasts about 2.8 ms and the whole control algorithm running on NiosII about 80 ms.

An experiment in which the robot faces with a complex environment is shown in Fig. 11.16 together with the corresponding evolution of the controlled multiscroll

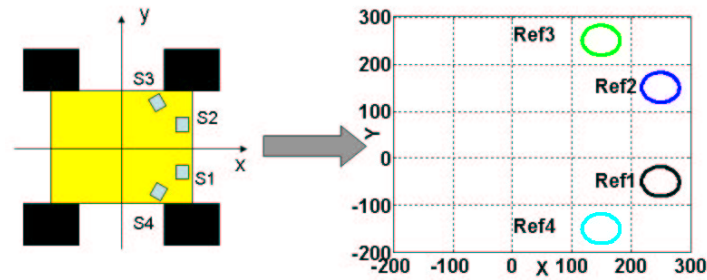


Fig. 11.15 Reference cycles representing the sensors of the robot.

system. Fig. 11.16 (a) and Fig. 11.16 (b) show a sensor output; a high value means a low distance from an obstacle. The sample time is about 0.350 s. In Fig. 11.16 (c) the robot senses an obstacle on the right side; both sensors S1 and S4 are activated but in a different way: the control gain associated with S4 is higher than the other gain. Therefore, the resulting cycle is placed between Ref1 and Ref4 but closer to Ref4 (Fig. 11.16 (d)). In this case the robot turns in the opposite direction, and the speed and rotation angle depend on the characteristics of the emerged cycle. Subsequently, the sensors do not see any obstacle (Fig. 11.16 (e)), so the multiscroll system shows a chaotic behavior (Fig. 11.16 (f)) and the robot continues to explore the environment, moving with constant speed and without modifying its orientation. In the last picture, Fig. 11.16 (g), only S1 sensor is slightly activated, so the emerged cycle is placed on the reference Ref1 although a small control gain is used (Fig. 11.16 (h)).

Another experiment, whose video is reported in [8], shows the robot in an arena. It continuously explores the environment until it finds an exit.

As performed for the simulated robot, also with the real one we made a series of tests in two different environments (Fig. 11.17). Five experiments for each arena have been carried out placing the robot in a random initial position. An example of the trajectory followed in each environment by the robot controlled through the WCC_f method is shown in Fig. 11.17.

In each experiment the robot explores the environment for 7 minutes. The behaviour of the robot has been recorded through a video camera. A movie, has been used to extract the robot trajectory and to evaluate the explored area. The results obtained in the two arenas are shown in Fig. 11.18. In this case the WCC_f algorithm was selected to be experimentally shown. From the analysis of Fig. 11.18 the capability of the algorithm to densely explore the environment in a few minutes can be appreciated.

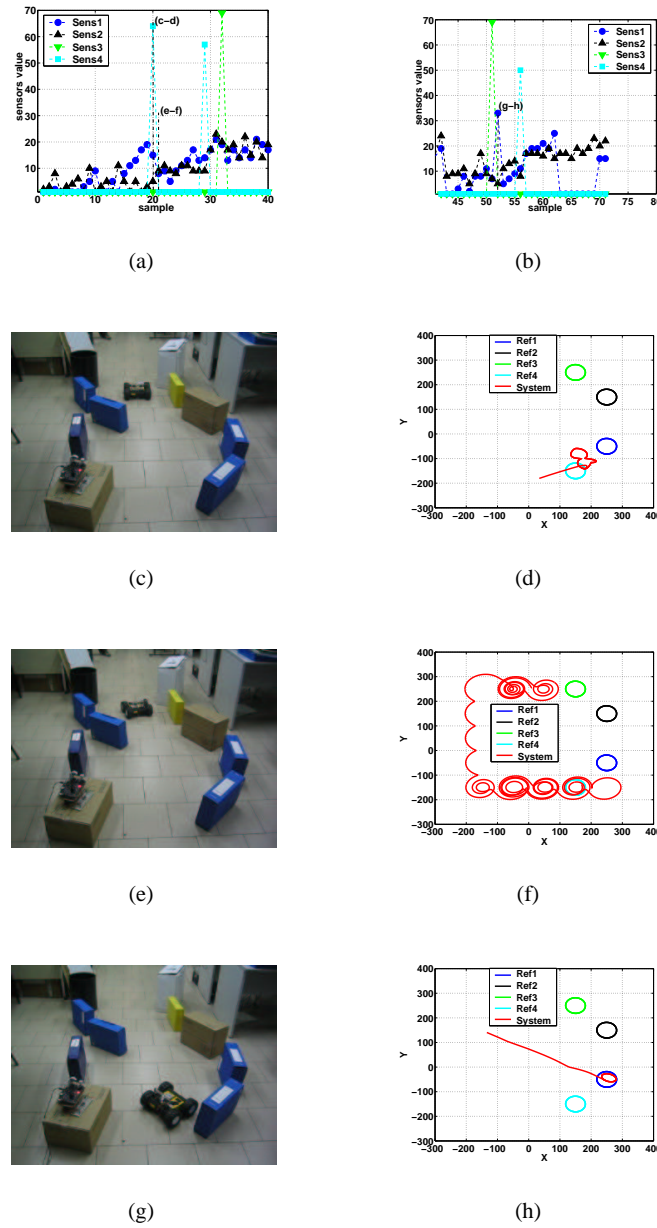


Fig. 11.16 Screen shots of the robot during the exploration of an unknown environment and the evolution of the controlled multiscroll system. (a)(b) Sensory signals acquired during the experiment with a sample time of about 0.350 s; the acquired infrared sensor output reported on the y-axis goes from 0 to 70 that correspond to a distance from 80 cm to 25 cm. (c)(d) More than one sensor is concurrently active. (e)(f) No obstacle is considered relevant for the robot movement. (g)(h) The right sensor (S3) detects an obstacle.

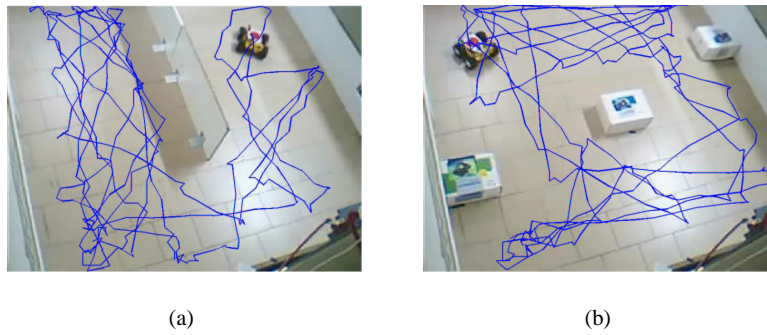


Fig. 11.17 Environments used to evaluate the performance of the proposed architecture controlling a roving robot. The dimensions of both arenas are 10x10 robot units. An example of the trajectory followed by the robot controlled through the WCC_f algorithm is shown.

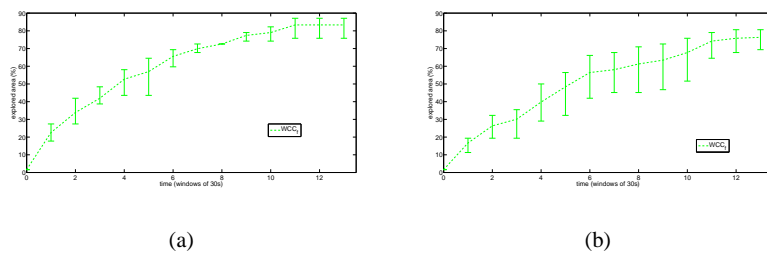


Fig. 11.18 Area explored for the environments shown in Fig. 11.17 (a) and (b). The arena whose dimension is 10x10 robot units, has been divided into locations of 1x1 robot units. The experiment time is 420s and the mean value of area explored, mediated over 5 experiments, calculated with time windows of 30s, is indicated. The bars show the minimum and maximum value.

11.4.5 Learning anticipation via spiking networks

Objectives: A roving robot is engaged in learning how to deal with higher level sensors by using, as teaching signals, those coming from low level sensors. The learning paradigm used is the Spike Timing Dependent Plasticity (STDP).

Experimental set-up: Rover I is equipped with the Eye-RIS v1.1 in frontal configuration, distance sensors and low level target sensors. The arena contains obstacles and two black circles on the ground that are used as targets.

Results:

The problem of correlation among different sensory stimuli and the possibility to anticipate events has been discussed in Chapter 6. The control architecture, based on a spiking network and implemented on the SPARK hardware, is here applied to Rover I.

The results that we are here reporting demonstrate how the robot is able:

- to learn distance sensors based on information coming from contact sensors (here simulated using short range sensors), that represent unconditioned stimuli;
- to learn visual qualities related to an object and correlating them to information related to a target sensor. In our demo the target sensor is a light sensor, positioned in the bottom part of the robot, facing the ground, while the conditioned sensor is a visual one (the Eye-RIS v1.2 was used).

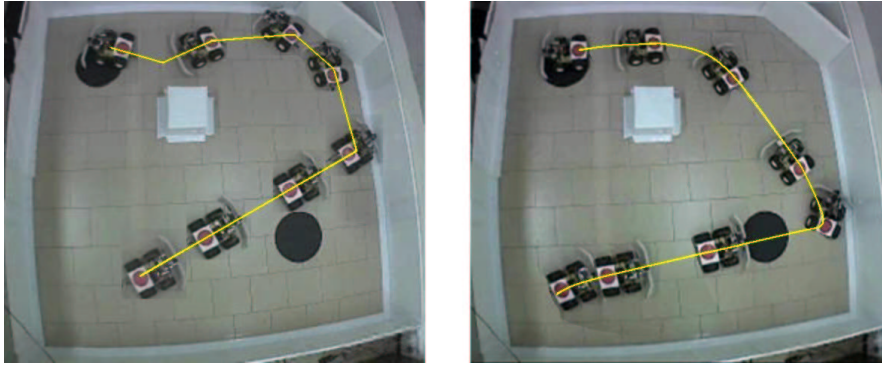


Fig. 11.19 Trajectories before and after learning with Rover I.

In Fig. 11.19, the trajectory followed by the robot at the beginning and after 30 minutes of learning is reported. As can be easily seen, the robot learnt through its basic behaviours (i.e. collision reaction and low level target attraction) how to deal with other more complex stimuli as the visual one, in order to improve its capabilities. The improvement is quantitatively summarized in Fig. 11.20 in which the decrement of the number of bumps and the increment in terms of number of targets found during the learning phase is shown.

11.4.6 Landmark navigation

Objectives: The focus of this demo is to outline the robot capability to learn to discriminate between relevant and useless pictures in the arena. The relevant pictures can work as landmarks for homing purpose. Once learned the landmarks, homing takes place exploiting the MMC recurrent network, even in front of partially obscured landmarks.

Experimental set-up: Rover II is equipped with the Eye-RIS v1.2, distance sensors and low level target sensors. The arena contains a target (i.e. nest) and five different possible landmarks (i.e. black picture frame with objects inside, attached to the walls).

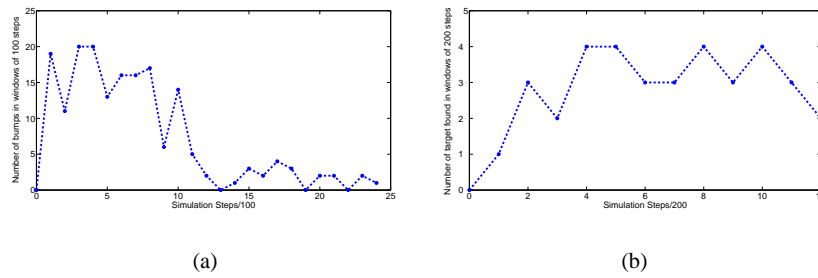


Fig. 11.20 Learning obstacle avoidance and target retrieving through STDP. (a) Number of bumps occurred in time windows of 100 steps, (b) number of targets found in time windows of 200 steps.

Results:

The landmark navigation algorithm, as discussed in Chapter 6, is characterized by two distinct phases.

Phase I: Landmark identification

In this phase, the roving robot randomly explores the arena filled with different types of visual cues. At each step the robot acquires information about the presence of different visual cues, provided by the Eye-RIS v1.2. The robot is also able to detect the presence of the nest only within its proximity. The most reliable visual cues (three in our demo) will have, at the end of the learning phase, the highest values for their synaptic weights (through STDP learning), and will be selected as landmarks for the next phase. The arena used for the experiments is shown in Fig. 11.21.



Fig. 11.21 Environment used for landmark navigation.

Phase II: Landmark navigation

In this phase the roving robot, placed on the nest position, acquires, via the Eye-RIS v1.2 and a compass sensor, information about the three most reliable landmarks, discovered in the previous phase, in order to build a map of the geometrical relationships between landmarks and nest. The comparison between the real map and the map generated by the algorithm is shown in Fig. 11.22 and relevant data are summarized in Table 11.1. The error due to measurement noise (in particular on the compass sensor) is not a problem for the navigation algorithm, thanks to the filtering capabilities of the RNN structure.

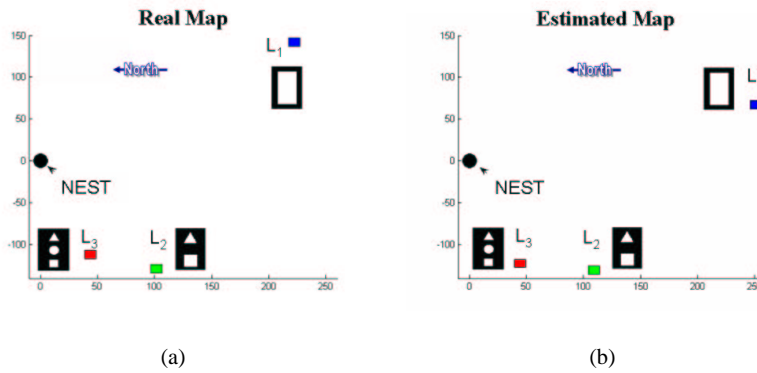


Fig. 11.22 Map reconstruction for landmark navigation. (a) real map, (b) map generated using sensory data acquired through a compass sensor and the Eye-RIS v1.2 visual system.

Table 11.1 Comparison between the real map and the map estimated through data acquired by using compass sensor and visual system. Angles are calculated in degrees with respect to the south direction whereas distance is in cm.

Landmark	Real				Estimated			
	Dist	Ph	X	Y	Dist	Ph	X	Y
L_1	260	147	251	67	264	165	222	142
L_2	170	-128	109	-130	164	-130	101	-129
L_3	130	-111	44	-122	120	-110	44	-112

After that, we let the robot forage for some steps and, once it needs to come back to the nest, it turns around looking for a landmark. The information (distance and angle) of the relative position between robot and landmark is acquired via the visual system and enters in the RNN. The RNN output is a vector which is translated in a motor command. After some iterations, the rover will reach the nest position (see Fig. 11.23).

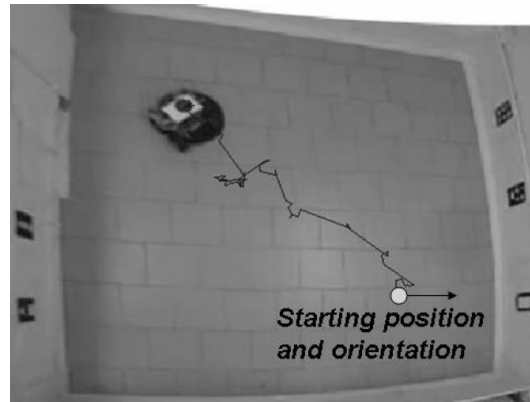


Fig. 11.23 Trajectory followed by the robot guided by the reliable landmarks.

11.4.7 Turing Pattern Approach to perception

Objectives: The roving robot is able to autonomously learn navigation strategies, through the emergence of Turing Pattern in the SPARK hardware. The perceptual model shapes, through learning, the basins of attraction of each pattern to account for the environmental needs.

Experimental set-up: Rover I is equipped with distance sensors and a compass sensor. The perceptual core was designed in VHDL and implemented in the SPARK board.

Results:

The cognitive architecture based on the Turing Pattern Approach (TPA) has been already discussed in Chapter 7. One of the key point of this control architecture consists in the hardware implementation of the whole sensing-perception-action loop. Fig. 11.24 shows the hardware scheme. The perceptual core, dedicated to the Turing patterns generation, has been completely developed in VHDL, whereas the action system together with the interface with the Rover has been realized by using the Nios II soft-core microprocessor (i.e. programmed in C++ language).

The low level hardware implementation of the perceptual core represents the final result of an optimization process. The first implementation step was devoted to validate the correctness of the algorithm; to do that on the Spark board, the Nios II development environment has been chosen. The results were good in term of hardware resources needed, but not feasible for real-time application due to a computational time of about 90 seconds. To improve this results, custom instructions (i.e. dedicated hardware modules for floating point operations) were introduced in the code obtaining a decrement of about 50% with respect to the standard Nios code. Aiming at reach a control loop time under one second (i.e. orders of magnitude under the obtained time), a VHDL implementation was taken into consideration. The final hardware design is able to elaborate Turing Patterns in no more than 98 ms without

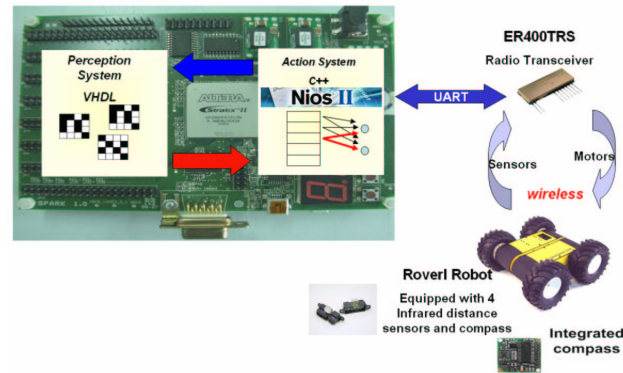


Fig. 11.24 Control scheme for the Turing Pattern Approach.

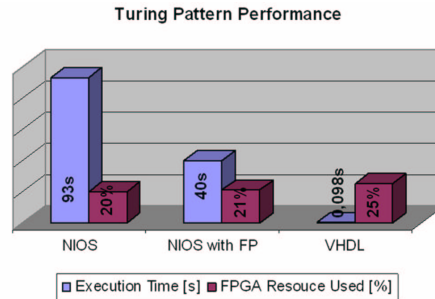


Fig. 11.25 Performances of different TPA implementations on the SPARK board.

exceeding in resources needed, that are under the 25% of the total. A comparison between the different implementation strategies is reported in Fig. 11.25.

In order to show the performance of the roving robot controlled through the TPA implemented on the SPARK board, the rover was placed in a arena whose dimensions are $3 \times 3 \text{ m}^2$, filled with 3 obstacles in addition to the walls. The mission assigned to the robot consists into follow a target direction avoiding obstacles.

Fig. 26(a) shows the cumulative number of new patterns emerging during the learning phase. It is evident how the total number of emerged patterns is constant after about 800 learning cycles. In the experiment here reported, the robot can use about 30 different patterns to specialize its behavior depending on the environment conditions. All the possible actions, that the robot can perform at the end of the learning phase, are shown in Fig. 26(b).

An example of the robot behavior is shown in Fig. 11.27 in which the trajectory followed by the roving robot is reported together with the different Turing patterns that constitute the specific internal representations of the robot surroundings as learned during the learning phase.

Finally, Fig. 11.28 shows all the Turing patterns used in the previous trajectory, reporting for each pattern the number of occurrences and the associated action.

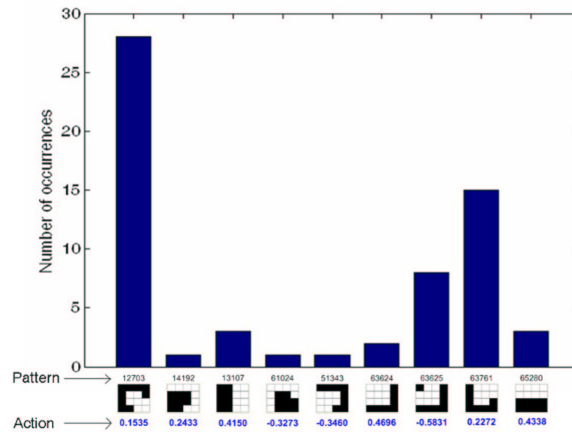


Fig. 11.28 Number of occurrences for each Turing pattern in the previously shown trajectory. The action, in term of turning angle, associated with each pattern are also reported in radians.

11.4.8 Representation layer for Behaviour Modulation

Objectives: Here Turing Patterns are used to provide no longer a single action at the output stage, but to modulate the basic behavior responses in the pre-motor area. A roving robot will be used as a demonstrator of the learning phase executed on the PC.

Experimental set-up: Rover II is equipped with distance sensors, a compass sensor and the hearing board. The emulated lower level basic behaviors are:

- phonotaxis;
- optomotor reflex;
- obstacle avoidance reflex.

Results:

The experiments have been carried out within a $3 \times 3 m^2$ arena where two obstacles and a sound source have been placed (Fig. 11.29). In the experiments, we test the architecture with the learned modulation parameters compared with the case of fixed modulation. For each case, we let the robot perform three trials starting from the same position. Fig. 11.30 shows the trajectory followed in the best and in the worst trial for the two cases under analysis, while Fig. 11.31 reports the path length

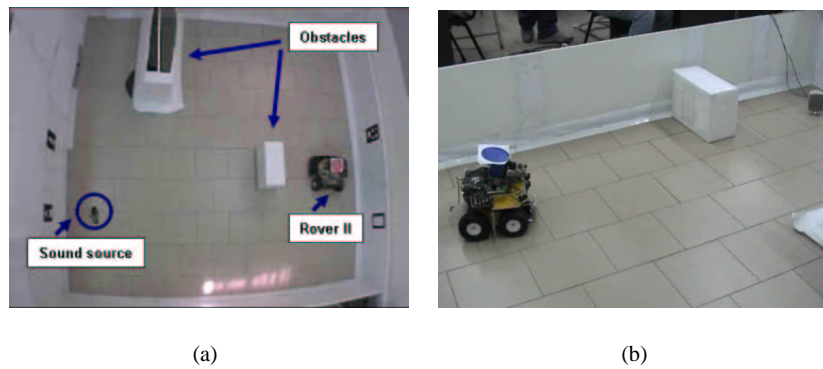


Fig. 11.29 (a) Experimental set-up (b) Rover II navigates in the arena.

for all the trials. As well as in the simulations reported in Chapter 7, in the presented experiments, the performance increase is evident in terms of path length to reach the target and robustness of the behavior against noise sources introduced in the environment. The behaviour robustness is confirmed by the low variance in the path length along the different trials.

Multimedia material, including tests in very noisy and dynamically changing environments, is available in [8].

11.5 Conclusion

The emergence of cognitive capabilities in artificial agents is one of the big challenges of our decades. Different directions are currently followed by researchers trying to develop artificial cognitive agents.

This chapter gives a contribution to this research activity proposing a series of experiments that underline some of the potential applications of the SPARK architecture. These results do not represent the end of a path but just the beginning of an activity devoted to improve the preliminary results here proposed to further generalize the application capabilities and its fields of application.

Acknowledgements Authors acknowledge the support of STMicroelectronics for supplying technical help, microcontrollers and boards useful for the realization of Rover II.

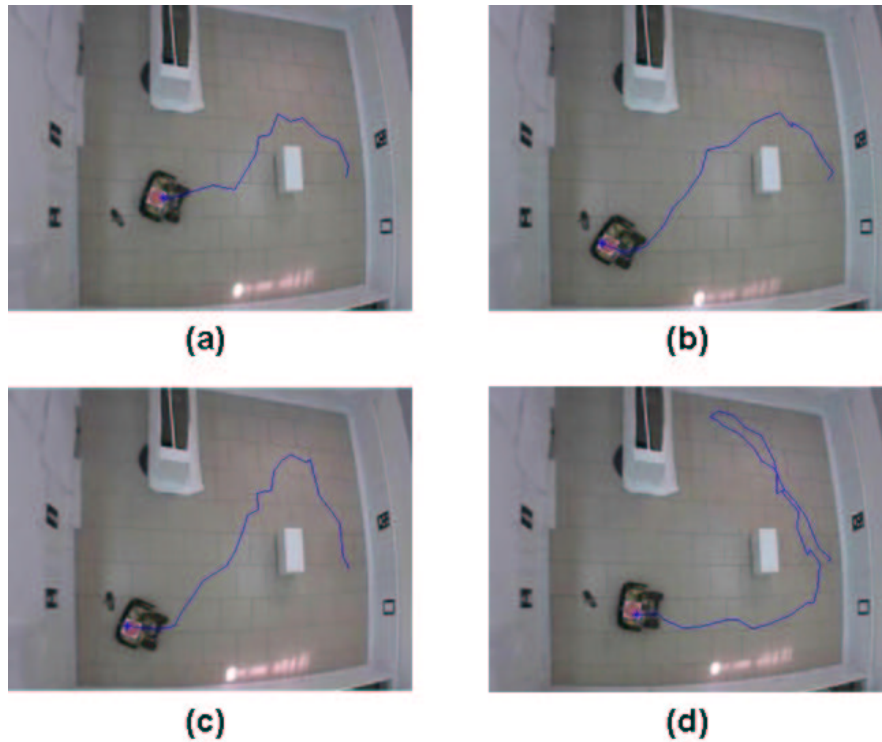


Fig. 11.30 Best and worst trial in the case of learned ($a-b$) and constant ($c-d$) modulation.

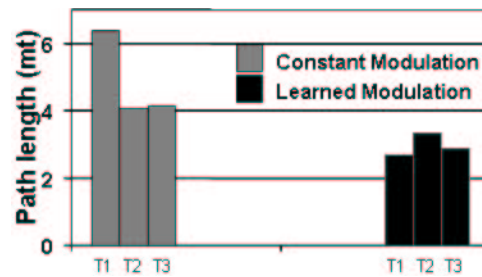


Fig. 11.31 Path length for all the experiments with the roving robot.

References

1. Arena, P., Fortuna, L., Frasca, M., Patané, L.: Sensory feedback in CNN-based central pattern generators. *International Journal of Neural Systems* **13**(6), 349–362 (2003)
2. Arena, P., Fortuna, L., Frasca, M., Patané, L., Pollino, M.: An autonomous mini-hexapod robot controlled through a CNN-based CPG VLSI chip. In: *Proc. of CNNA*, pp. 401–406, Istanbul, Turkey (2006)
3. Arena, P., De Fiore, S., Fortuna, L., Nicolosi, L., Patané, L., Vagliasindi, G.: Visual Homing: experimental results on an autonomous robot. In: *18th European Conference on Circuit*

- Theory and Design (ECCTD 07), Seville, Spain (2007)
4. Arena, P., Patané, L., Schilling, M., Schmitz, J.: Walking capabilities of Gregor controlled through Walknet. In: Proc. of Microtechnologies for the New Millennium (SPIE 07), Gran Canaria, Spain (2007)
 5. Arena, P., De Fiore, S., Fortuna, L., Frasca, M., Patané, L.: Reactive navigation through multiscroll systems: from theory to real-time implementation. *Autonomous Robots*. ISSN: 0929-5593. doi:10.1007/s10514-007-9068-1 Published on-line (2008).
 6. Braitenberg, V.: *Vehicles: experiments in synthetic psychology*. MIT Press, Cambridge, MA (1984)
 7. Cruse, H., Durr, V., Schmitz, J.: Insect walking is based on a decentralised architecture revealing a simple and robust controller. *Phil. Trans. R. Soc. Lond. A* **365**(1850), 221–250 (2006)
 8. Robot Multimedia material, Webpage available on line at www.spark.diees.unict.it/Robot.html